The complete mitochondrial genomes of five longicorn beetles (Coleoptera: Cerambycidae) and phylogenetic relationships within Cerambycidae

Jun Wang [1] , **Xin-Yi Dai** [1] , **Xiao-Dong Xu** [1] , **Zi-Yi Zhang** [1] , **Dan-Na Yu** [1, 2] , **Kenneth B Storey** [3] , **Jia-Yong Zhang** [Corresp. 1, 2]

1 College of Chemistry and Life Science, Zhejiang Normal University, Jinhua, Zhejiang, China

2 Key lab of wildlife biotechnology, conservation and utilization of Zhejiang Province, Zhejiang Normal University, Jinhua, Zhejiang, China

3 Department of Biology, Carleton University, Ottawa, Ontario, Canada

Corresponding Author: Jia-Yong Zhang
Email address: zhangjiayong@zjnu.cn

Cerambycidae is one of the most diversified groups within Coleoptera and includes nearly 35,000 known species. The relationships at the subfamily level within Cerambycidae have not been convincingly demonstrated and the gene rearrangement of mitochondrial genomes in Cerambycidae remains unclear due to the low numbers of sequenced mitogenomes. In the present study, we determined five complete mitogenomes of Cerambycidae and investigated the phylogenetic relationship among the subfamilies of Cerambycidae based on mitogenomes. The mitogenomic arrangement of all five species was identical to the ancestral Cerambycidae type without gene rearrangement. Remarkably, however, two large intergenic spacers were detected in the mitogenome of *Pterolophia* sp. ZJY-2019. The origins of these intergenic spacers could be explained by the slipped-strand mispairing and duplication/random loss models. A conserved motif was found between *trnS2* and *nad1* gene, which was proposed to be a binding site of a transcription termination peptide. Also, tandem repeat units were identified in the A+T-rich region of all five mitogenomes. The monophyly of Lamiinae and Prioninae was strongly supported by both MrBayes and RAxML analyses based on nucleotide datasets, whereas the Cerambycinae and Lepturinae were recovered as non-monophyletic.

1 **The complete mitochondrial genomes of five longicorn beetles**

2 **(Coleoptera: Cerambycidae) and phylogenetic relationships within**

3 **Cerambycidae**

4 Jun Wang[1], Xin-Yi Dai[1], Xiao-Dong Xu[1], Zi-Yi Zhang[1], Dan-Na Yu[1,2], Kenneth B. Storey[3], Jia-

5 Yong Zhang[1,2]

7 *[1] College of Chemistry and Life Science, Zhejiang Normal University, Jinhua, 321004, Zhejiang*

8 *Province, China*

9 *[2] Key lab of wildlife biotechnology, conservation and utilization of Zhejiang Province, Zhejiang*

10 *Normal University, Jinhua, 321004, Zhejiang Province, China*

11 *[3] Department of Biology, Carleton University, Ottawa, Ontario, K1S5B6, Canada*

13 Corresponding author: JY Zhang: zhang3599533@163.com or zhangjiayong@zjnu.cn

15 Other authors:

16 J Wang: 17388152521@163.com

17 XY Dai: kkr_xy@163.com

18 XD Xu: ki01110015@163.com

19 ZY Zhang: cixi55@126.com

20 KB Storey: kenneth.storey@carleton.ca

21 DN Yu: ydn@zjnu.cn

26 **ABSTRACT**

27 Cerambycidae is one of the most diversified groups within Coleoptera and includes nearly

28 35,000 known species. The relationships at the subfamily level within Cerambycidae have not

29 been convincingly demonstrated and the gene rearrangement of mitochondrial genomes in

30 Cerambycidae remains unclear due to the low numbers of sequenced mitogenomes. In the

31 present study, we determined five complete mitogenomes of Cerambycidae and investigated the

32 phylogenetic relationship among the subfamilies of Cerambycidae based on mitogenomes. The

33 mitogenomic arrangement of all five species was identical to the ancestral Cerambycidae type

34 without gene rearrangement. Remarkably, however, two large intergenic spacers were detected

35 in the mitogenome of *Pterolophia* sp. ZJY-2019. The origins of these intergenic spacers could be

36 explained by the slipped-strand mispairing and duplication/random loss models. A conserved

37 motif was found between *trnS2* and *nad1* gene, which was proposed to be a binding site of a

38 transcription termination peptide. Also, tandem repeat units were identified in the A+T-rich

39 region of all five mitogenomes. The monophyly of Lamiinae and Prioninae was strongly

40 supported by both MrBayes and RAxML analyses based on nucleotide datasets, whereas the

41 Cerambycinae and Lepturinae were recovered as non-monophyletic.

42

43 **Keywords:** Mitochondrial genome, Cerambycidae, Intergenic spacer, Phylogenetic relationship
44

の

46

INTRODUCTION

47

48   Coleoptera (Hexapoda: Insecta) are a highly diverse group of insects consisting of about

49   360,000 known species of beetles that account for almost 40% of all described insect species

50   (*Lawrence & Newton, 1982; Hunt et al., 2007*). Cerambycidae (longicorn beetles) is one of the

51   species-rich families of Coleoptera and is a group of phytophagous insects with over 4000 genera

52   and 35,000 species in the world (*Monné ML, Monné & Mermudes, 2009; Sama et al., 2010*).

53   Longicorn beetles are morphologically and ecologically diverse, and have significant effects on

54   almost all terrestrial ecosystems (*Ponomarenko & Prokin, 2015*). Nevertheless, owing to their

55   remarkable species richness, variable morphological features and sparse gene data, the resolution

56   of the phylogeny of longicorn beetles has turned out to be a difficult challenge (*Bologna et al.,*

57   *2008; Zhang et al., 2018c*). Cerambycidae *s. s.* (sensu stricto) has usually been divided into eight

58   subfamilies: Lamiinae, Cerambycinae, Lepturinae, Prioninae, Dorcasominae, Parandrinae,

59   Spondylidinae and Necydalinae (*Svacha, Wang & Chen, 1997*) whereas Cerambycidae *s. l.*

60   (sensu lato) was considered to consist of Cerambycidae *s. s.*, Disteniidae, Oxypeltidae and

61   Vesperidae (*Napp,1994; Reid, 1995; Svacha, Wang & Chen, 1997*). Even if the number and

62   definition of Cerambycidae gradually stabilizes, the relationships at the subfamily level remained

63   unclear.

64   The mitochondrial genome is widely considered to be an informative molecular marker for

65   species identification, molecular evolution, and comparative genomic research (*Moritz, Dowling*

66   *& Brown, 1987; Boore, 1999*) due to its maternal inheritance and high evolutionary rate

67   properties (*Avise et al., 1987*). In the last few years, studies of animal mitogenomes have grown

68   rapidly in number and approximately 40,000 mitogenome sequences have now been published in

69   the NCBI database (*Tan et al., 2017*). By contrast, a mere 18 sequenced mitogenomes of

70   Cerambycidae have been reported, among them being eight mitogenomes belonging to the

71   subfamily Lamiinae, four mitogenomes of the subfamily Cerambycinae, three mitogenomes of

72   the subfamily Prioninae, and three mitogenomes of the subfamily Lepturinae (*Kim et al., 2009;*

73 *Chiu et al., 2016; Fang et al., 2016; Guo et al., 2016; Li et al., 2016a; Li et al., 2016b; Wang et*

74 *al., 2016; Lim et al., 2017; Liu et al., 2017; Song et al., 2017; Liu et al., 2018; Que et al., 2019;*

75 *Wang et al., 2019*). These few mitogenomes seriously restrict the capacity for phylogenetic

76 analyses and phylogeography of the Cerambycidae.

77 The gene organization of the known mitogenomes of Coleoptera, especially the

78 arrangements of protein-coding genes, are mostly in accordance with those of ancestral insects

79 (*Timmermans, Martijn & Vogler, 2012*). Nevertheless, recent evidence suggested that gene

80 rearrangements had occurred in the tRNA of *Mordella atrata* (Coleoptera: Mordellidae) and

81 *Naupactus xanthographus* (Coleoptera: Curculionidae) (*Song et al., 2010*). In addition to these,

82 recombination in the control region was observed in *Phrixothrix hirtus* (Coleoptera:

83 Phengodidae) and *Teslasena femoralis* (Coleoptera: Elateridae) (*Amaral et al., 2016*). The

84 mitogenome structure was originally found with no introns, sparse intergenic spacers and no

85 overlapping genes (*Ojala, Montoya & Attardi, 1981*). Nevertheless, large non-coding regions

86 (except the A+T-rich region) in mitogenomes have been observed within beetles, including a

87 1724-bp long intergenic spacer region in *Pyrocoelia rufa* (Coleoptera: Lampyridae), a 494-bp

88 region in *Hycleus chodschenticus* (Coleoptera: Meloidae) and two large intergenic spacers of

89 more than 30 bp in *Hycleus* species (*Bae et al., 2004; Yuan et al., 2016; Haddad et al., 2018*).

90 Previously reported tandem repeat units or an additional origin of replication were identified

91 among large intergenic regions (*Dotson & Beard, 2001; Rodovalho et al., 2014*).

92 The phylogenetic relationships within Cerambycidae have yet to be fully resolved due to a

93 lack of adequately convincing taxon sampling, and the monophyly of subfamilies within

94 Cerambycidae need further discuss (*Haddad et al., 2018; Kim et al., 2018*). With the aim to

95 discuss the monophyly of subfamilies of Cerambycidae and gene arrangements of the

96 mitogenome, complete mitogenomes of the five longicorn beetle species were determined. We

97 also described the structural and compositional features of the newly sequenced mitogenomes

98 and analyzed the intergenic spacers to explain the possible evolutionary mechanisms.

99 **MATERIALS AND METHODS**

Sampling collection and DNA extraction

Five longicorn beetle specimens (*Oberea yaoshana*, *Thermistis croccocincta*, *Blepephaeus succinctor*, *Nortia carinicollis*, *Pterolophia* sp. ZJY-2019) were captured from Jinxiu, Guangxi Zhuang Autonomous Region, China and were stored at −40 °C in the lab of JY Zhang (College of Chemistry and Life Science, Zhejiang Normal University). The specimens were identified by Dr. JY Zhang based on morphology. Total genomic DNA was extracted from the thorax muscle using Ezup Column Animal Genomic DNA Purification Kit (Sangon Biotech Company, Shanghai, China).

PCR amplification and sequencing

In order to obtain the entire mitogenome of samples, we used eleven universal primer pairs to amplify eleven adjacent and overlapping fragments (*Simon et al., 2006; Zhang et al., 2008; Zhang et al., 2018a, 2018b*). Then specific primers were designed from the initial overlapping fragments using Primer Premier 5.0 (Premier Biosoft International, Palo Alto, CA). A total of 45 pairs of primers were used in the present study to amplify and sequence the remaining gaps (Table S1). The cycling conditions and reaction volume of PCR amplifications were as in *Cheng et al. (2016)* and *Gao et al. (2018)*. All PCR products were sequenced by Sangon Biotech Company (Shanghai, China).

Mitogenome annotation and sequence analyses

Manual proofreading and assembling of contiguous and overlapping sequences used DNASTAR Package v.6.0 (*Burland, 2000*). We annotated the tRNA genes by MITOS (freely available at http://mitos.bioinf.uni-leipzig.de/index.py) (*Bernt et al., 2013*). Two rRNA genes and the A+T-rich region were identified using the Clustal W in Mega 7.0 (*Kumar, Stecher & Tamura, 2016*) based on alignments of homologous sequences from other species of Cerambycidae available in the GenBank (*Kim et al., 2009; Fang et al., 2016; Lim et al., 2017*). The nucleotide sequences of the 13 protein-coding genes (PCGs) were translated into amino acids based on the invertebrate mitogenome genetic code (*Cameron, 2014*). We used Mega 7.0 (*Kumar, Stecher & Tamura, 2016*) to find the open reading frames of the 13 PCGs and calculate

129   AT content along with codon usage for the five newly sequenced mitogenomes. Circular

130   mitogenome maps were generated by CG View server V 1.0 (*Grant & Stothard, 2008*).

131   Composition skew analysis was calculated on the basis of the formula AT-skew = (A − T)/(A +

132   T) and GC-skew = (G − C)/(G + C) (*Perna & Kocher, 1995*). Tandem Repeat Finder V 4.07

133   (http://tandem.bu.edu/trf/trf.html) (*Benson, 1999*) was used to find tandem repetitive sequences.

134

135   **Phylogenetic analyses**

136   For the purpose of reconstructing the phylogenetic relationships of Cerambycidae, a

137   nucleotide dataset (13P26) of the 13 protein-coding genes of 26 complete mitogenomes was used

138   (Table 1) according to the methods of *Zhang et al. (2019)*, this included the 5 newly determined

139   sequences and 18 published complete mitogenomes of Cerambycidae (*Kim et al., 2009; Chiu et*

140   *al., 2016; Fang et al., 2016; Guo et al., 2016; Li et al., 2016a; Li et al., 2016b; Wang et al.,*

141   *2016; Lim et al., 2017; Liu et al., 2017; Song et al., 2017; Liu et al., 2018; Que et al., 2019;*

142   *Wang et al., 2019*). Three species of Galerucinae, *Paleosepharia posticata*, *Diabrotica barberi*

143   and *Diabrotica virgifera* served as the out-groups (*Coates & Brad, 2014; Wang & Tang, 2017*).

144   To verify whether the lack of samples affects the relationships among the Cerambycidae, we

145   reconstructed Cerambycidae phylogeny based on the nucleotide data (12P38) of 12 PCGs

146   (omitting the *nad2* gene) from 38 complete or nearly complete mitogenomes (Table 1). These

147   include all species of the 13P26 dataset, 8 directly submitted partial mitogenomes of

148   Cerambycidae, one mitogenome of Necydalinae, two mitogenomes of Vesperidae and one

149   mitogenome of Disteniidae (*Nie et al., 2017*). Each of the 13 protein-coding genes in 13P26

150   dataset or 12 protein-coding genes in 12P38 dataset was aligned using Clustal W in the program

151   Mega 7.0 (*Kumar, Stecher & Tamura, 2016*). Conserved regions were identified by the program

152   Gblock 0.91b (*Castresana, 2000*). Protein-coding genes were partitioned a priori by codon

153   position. Accodrding to the analyses methods of *Zhang et al. (2008)*, *Ma et al. (2015)* and *Cheng*

154   *et al. (2016)*, we excluded the third codon positions because of the saturated third codon

155   positions and obtained a 12P38 dataset with 5584 nucleotide sites and 13P26 dataset with 6960

156   nucleotide sites. So 12P38 dataset with 24 partitions and 13P26 dataset with 26 partitions were

157 used. The optimal partitioning scheme and best-fitting models were selected by the program

158 PartitionFinder 1.1.1 (*Lanfear et al., 2012*) based on the Bayesian information criterion (BIC)

159 (Table 2 and Table 3). Bayesian Inference (BI) and Maximum likelihood (ML) methods were

160 used for phylogenetic analyses. BI analyses were carried out in MrBayes 3.2 (*Ronquist et al.,*

161 *2012*) with the model of GTR + I + G. The runs were set for 10 million generations with

162 sampling every 1,000 generations. The first 25% of generations were removed as burn-in and the

163 average standard deviation of split frequencies in Bayesian was below 0.01. ML analyses were

164 performed by RAxML 8.2.0 with the best-fitting model of GTRGAMMAI. Branch support

165 values were inferred from a rapid bootstrap method applied with 1,000 replications (*Stamatakis,*

166 *2014*).

167

RESULTS AND DISCUSSION

Mitogenome organization and composition

170 In this study, the complete mitogenomes of five species of the subfamilies Cerambycinae

171 and Lamiinae (*O. yaoshana, T. croccocincta, B. succinctor, N. carinicollis, Pterolophia* sp. ZJY-

172 2019) were determined. Structures of the five newly sequenced entire mitogenomes are shown in

173 Fig. S1-S5. The lengths of the five mitogenomes were basically within the range of the published

174 Cerambycidae species in the GenBank database, covering sizes between 15,503 bp in *T.*

175 *croccocincta* to 16,063 bp in *Pterolophia* sp. ZJY-2019. Every mitogenome of the five species

176 possessed similar compositional profiles and featured the typical gene arrangement and

177 orientation that have been hypothesized for most coleopteran insects (*Wolstenholme, 1992;*

178 *Boore, Lavrov & Brown, 1998*), with the *trnW-trnC-trnY* triplet (Table S2-S6). Twenty-three

179 genes were coded on the majority strand (J-strand), with the remaining fourteen genes coded on

180 the minority strand (N-strand) (Fig. S1-S5). The nucleotide composition of the five longicorn

181 beetle mitogenomes was strongly biased towards A and T, which made up 73.2% (*N. carinicollis*)

182 to 79.1% (*O. yaoshana*) of the base pairs. A comparison of AT-skew and GC-skew showed that

183 the AT skew of all mitogenomes was positive and the GC-skew was negative (Table 4).

184 **Protein-coding genes and codon usages**

185   The orientations of the 13 the PCGs of the five longicorn beetles were identical to most

186 coleopteran species (Table S2-S6). Conventional initiation codons were assigned to the majority

187 of the PCGs, except for *nad1*, which started with TTG in all five beetles. Most putative protein

188 sequences showed typical stop codons (TAA/TAG), but the *nad4* and *nad5* genes of *O. yaoshana*,

189 *T. croccocincta*, *B. succinctor* used a single T residue as the terminal codon. The *cox1* and *cox2*

190 genes of *O. yaoshana*, *T. croccocincta* and *Pterolophia* sp. ZJY-2019 also used a single T

191 residue as the terminal codon. Functional terminal codons can be produced by partial terminal

192 codons in polycistronic transcription cleavage and polyadenylation processes (*Anderson et al.,*

193 *1981; Ojala, Montoya & Attardi, 1981; Du et al., 2016*). The relative synonymous codon usage

194 (RSCU) of the five Cerambycidae mitochondrial genomes was calculated (Fig. 1, Table S7). The

195 results showed an over-utilization of A or T nucleotides in the third codon position as compared

196 to other synonymous codons, this is normally considered to be caused by genome bias, optimum

197 choice of tRNA usage or the benefit of DNA repair (*Chai & Du, 2012; Ma et al., 2015*).

198   Comparative analyses also indicated that the major customarily utilized codons and the

199 codon usage patterns of the five samples were conservative. For instance, each of the five

200 mitogenomes possessed UUA (Leu), AUU (Ile), UUU (Phe), and AUA (Met) as the most

201 frequently used codons. All codons contained A or T nucleotides, indicating that the strong AT

202 mutation bias obviously influenced the codon usage (*Powell & Moriyama, 1997; Rao et al.,*

203 *2011*). Furthermore, the codons rich in AT encoded the most abundant amino acids, e.g. Leu

204 (15.6-16.4%), indicating that the AT bias also influences the amino acid constituents of the

205 proteins encoded by the mitochondrial genes (*Foster et al., 1997; Min & Hickey, 2007*).

206

207 **Ribosomal RNAs and transfer RNAs**

208   The two expected rRNAs (16S rRNA and 12S rRNA) were found in the mitochondrial

209 genomes of all five longicorn beetles. The 16S rRNA gene was situated between *trnL* and *trnV*

210 whereas the 12S rRNA gene was between *trnV* and the A+T-rich region. Due to the impossibility

211   of faultless determination by DNA sequence alone, the terminus of the rRNA genes in

212   coleopteran mitogenomes has been presumed to stretch to the border of the flanking genes

213   (*Boore, 2001*). Therefore, the 16S rRNA was presumed to fill the blank between *trnL* and *trnV*

214   whereas the border between 12S rRNA and the putative A+T-rich region was defined based on

215   alignments of homologous sequences of known longicorn beetles (*Boore & Brown, 2000*). The

216   sizes of 16S rRNA in the five beetle mitogenomes varied from 1261 bp for *N. carinicollis* to

217   1283 bp for *O. yaoshana*, and the sizes of 12S rRNA ranged between 759 bp for *Pterolophia* sp.

218   ZJY-2019 to 787 bp for *T. croccocincta*. These fit within the lengths detected in other

219   coleopteran mitogenomes. The A+T content of the rRNA genes was the highest (81.7%) in the

220   *Pterolophia* sp. ZJY-2019 mitogenome and the lowest in the *N. carinicollis* mitogenome (75.7%).

221   The AT-skew of 16S rRNA and 12S rRNA showed great positivity, whereas the GC-skew was

222   somewhat negative (Table 4), which indicated the occurrence of less As and Cs than Ts and Gs

223   (*Eyrewaker, 1997*).

224   The 22 typical tRNAs were detected in all five species like other published longicorn

225   beetles. All the anticodons were also highly conserved compared to other beetle species. Twenty-

226   two tRNAs excluding *trnS1* displayed the classic clover-leaf secondary structure, whereas *trnS1*

227   lacked the dihydrouridine (DHU) arm and formed a simple loop (Fig. S6). Nevertheless, this

228   abnormal tRNA has proven to be functional, although somewhat less effective than conventional

229   tRNAs (*Steinberg & Cedergren, 1994; Hanada et al., 2001; Stewart & Beckenbach, 2003*).

230   Another unusual feature was the use of TCT as the *trnS1* anticodon in Cerambycidae, whereas

231   most arthropods use a GCT anticodon in *trnS1*. In many other coleopteran mitogenomes the

232   *trnS1* anticodon (TCT) can also be observed (*Friedrich & Muqim, 2003; Bae et al., 2004*).

233   Mismatched pairs also exist in stems of tRNAs. For example, the mismatched pairs U-G existed

234   in the DHU stem of *trnY* and *trnQ*; U-U existed in the TΨC stem of *trnC* and in the anticodon

235   stem of *trnL1*; G-U existed in acceptor stem of *trnC*. It has been verified that mismatched pairs

236   can be revised via editing processes or may symbolize abnormal pairings (*Negrisolo, Babbucci*

237   *& Patarnello, 2011*).

238

239 **A+T-rich region**

240   A large non-coding region between 12S rRNA and *trnI*, ranging between 861 bp for *O.*

241 *yaoshana* to 1137 bp for *Pterolophia* sp. ZJY-2019, was found in the mitogenomes of the five

242 beetles. Owing to the high AT content levels of the overall mitogenome, this non-coding element

243 was defined as the A+T-rich region. It has been verified that the A+T-rich region harbors the

244 origin sites and essential regulatory elements for transcription and replication (*Wolstenholme,*

245 *1992; Taanman, 1999; Yukuhiro et al., 2002; Saito, Tamura & Aotsuka, 2005*). The sequence of

246 this region is relatively conserved owing to its high A+T content, and thus it is impossible to use

247 as a molecular marker (*Zhang & Hewitt, 1997*). The existence of tandem repeats in the

248 mitochondrial A+T-rich region has been observed in many coleopteran species. Some studies

249 such as that conducted by *Sheffield et al. (2008)* have shown that the A+T-rich region of

250 *Trachypachus holmbergi* (Coleoptera: Trachypachidae) possessed 21 similar copies of tandem

251 repeats consisting of a 58-bp fragment. The A+T-rich region of *Priasilpha obscura* (Coleoptera:

252 Phloeostichidae) is known to possess 6 tandem repeats of a 132-bp fragment and *Psacothea*

253 *hilaris* (Coleoptera: Cerambycidae) possesses 7 identical copies of a 57 bp tandem repeat (*Kim*

254 *et al., 2009*). In the present study, we found tandem repetitive sequences in all five newly

255 sequenced mitogenomes. The mitogenomes of *T. croccocincta* and *B. succinctor* contained three

256 copies of tandem repetitive sequences with lengths of 19 and 43 bp, respectively. Four tandem

257 repeats of a 19-bp fragment were found in the mitogenome of *Pterolophia* sp. ZJY-2019,

258 whereas two tandem repeats of a 25-bp fragment existed in *N. carinicollis*. The tandem repeats

259 generally exhibited high A+T contents. Moreover, two poly-T stretches were detected in the

260 mitogenome of *N. carinicollis*: one stretch was 16 bp in length (position: 14,880–14,895) near

261 the 12S rRNA gene and the other stretch was 17-bp in length (position: 15,283–15,299).

262 Previous studies have confirmed that the two poly-T stretches were structural signals for the

263 recognition of proteins that performed a role in replication initiation (*Andrews, Kubacka &*

264 *Chinnery, 1999*).

265

266 **Intergenic regions**

267   The mitogenomes of *O. yaoshana*, *T. croccocincta*, and *N. carinicollis* contain 6, 7, 9 non-

268   coding intergenic spacer sequences, with total lengths of 28 bp, 28 bp, and 31 bp, respectively,

269   whereas *B. succinctor* has 8 non-coding intergenic spacer sequences of 52 bp in total length.

270   Unexpectedly, a total of 354-bp of intergenic spacer, whose elements ranged from 1 to 184 bp in

271   length was found in the mitogenome of *Pterolophia* sp. ZJY-2019. The sequences are divided

272   into 9 regions, containing two large intergenic spacers. The largest one is 184 bp long situating

273   between *trnC* and *trnY*, and the other is 157 bp long situated between *trnS2* and *nad1* (Table S6).

274   Consequently, the total length of the mitogenome of *Pterolophia* sp. ZJY-2019 is longer than

275   that   of   other   longicorn   beetle   species.

276   The longer mitogenome length is due to the existence of its extended large intergenic spacers not

277   the A+T-rich region. Previously reported tandem repeat units or additional origins of replication

278   have been identified within this region (*Dotson & Beard, 2001; Rodovalho et al., 2014*). Proven

279   by the lack of introns, rare intergenic spacers, defective terminal codons and overlapping

280   fragments, mitogenomes characteristically show exceptional compactness of organization (*Ojala,*

281   *Montoya & Attardi, 1981*). Nevertheless, according to *Yuan et al. (2016)* and *Haddad et al.*

282   *(2018)*, large non-coding regions (except the A+T-rich region) in mitochondrial genomes were

283   observed in *Pyrocoelia rufa* (Coleoptera: Lampyridae) and some *Hycleus* species (Coleoptera:

284   Meloidae). Coincidentally, a 5 bp consensus motif (TACTA) exists in the intergenic regions

285   situated between *trnS2* and *nad1* of all five species studied here. This pentanucleotide motif is

286   conserved across coleopteran lineages (*Kim et al., 2009; Liu et al., 2018*), similar to the findings

287   that *Evania appendigaster* (Hymenoptera: Evaniidae) possessed a 6 bp motif 'THACWW' and

288   *Chilo suppressalis* (Lepidoptera: Pyralidae) possessed a 7 bp motif 'ATACTAA', respectively

289   *(Wei et al., 2010; Gong et al., 2018)*.

290   In the mitogenome of *Pterolophia* sp. ZJY-2019, the large intergenic region was situated

291   between *trnS2* and *nad1*, which included two copies of a 22 bp long consensus sequence

292   (TTACTAAATTTAATTAACTAAA) in both ends of the intergenic region. The formation of an

293   intergenic region may be explained by slipped-strand mispairing (*Levinson & Gutman, 1987; Du*

294   *et al., 2017*). Based on this theory, mispairing occurred during replication of DNA strands, and

295   what followed next was misaligned reassociation and then replication or repair was caused by

296   insertions of several repeat units. The resulting tandem repeat underwent random loss and/or

297   point mutation, with only the repeat units in both extremities remaining (Fig. 2a). However, a

298   tandem repeat was not found in the intergenic region located between *trnC* and *trnY* of

299   *Pterolophia* sp. ZJY-2019. We conjectured that some errors in DNA replication can lead to

300   tandem duplication in tRNA clusters *of trnW-trnC-trnY*, followed by the random loss of partial

301   duplicated genes, and leading to the large intergenic region formed by the residues (Fig. 2b). In

302   addition, *Hua et al. (2008)* suggested that the duplication-random loss model caused the

303   rearrangements in Hemiptera. *Du et al. (2017)* also suggested that the duplication-random loss

304   model was an evolutionary ancient mechanism in Coleoptera, which led to the random loss of

305   nucleotides.

306   Consequently, compared to the original tRNAs, the residual intergenic region was not

307   conserved. According to *Du et al. (2017)*, four species of *Hycleus* genera harbored similar

308   location and sequence of non-coding regions, which indicated that the region may serve as a

309   latent symbol to distinguish *Hycleus* from the other genera. Thus, we speculated the large

310   intergenic region of *Pterolophia* sp. ZJY-2019 may be a molecular feature in *Pterolophia*,

311   though we were unable to adequately confirm it owing to the lack of enough samples.

312

313   **Phylogenetic analyses**

314   The phylogenetic relationships were reconstructed based on the nucleotide data (13P26)

315   with BI and ML methods (Fig. 3). BI and ML phylogenetic analyses yielded a similar topology

316   except for the position of Lepturinae, which was in the sister group of (Cerambycinae +

317   Prioninae) with high values in BI, but supported as the basal group of Cerambycidae in ML

318   analyses. The BI tree indicated that Cerambycidae split into 2 major groups (0.73): a clade of

319   (Lepturinae + (Cerambycinae + Prioninae)) and a clade of Lamiinae. The monophyly of

320   Lamiinae, Lepturinae and Prioninae was supported by both BI and ML analyses, whereas the

321   monophyly of Cerambycinae was not recovered. Within the subfamily Lamiinae, the clade of

322 (Lamiinae + (*Batocera lineolata* + *Thyestilla gebleri*)) was supported. However, *Liu et al. (2018)*

323 favoured *T. gebleri* as the basal position of Lamiinae with a high value, and *B. lineolata* and

324 *Apriona swainsoni* were reliably recovered as a sister group. Our results concurred with the

325 suggestion that *B. lineolata* was closely related to *A. swainsoni*, rather than *T. gebleri*. The

326 results also placed *Pterolophia* sp. ZJY-2019 as a sister group of all remaining Lamiinae.

327 Moreover, our results suggested that *O. yaoshana* clustered with *Trachypachus holmbergi*, as a

328 sister group of *T. gebleri*. For the relationship within Cerambycinae, *M. raddei*, *A. oenochrous*

329 and *Obrium* sp. NS-2015 were gathered into one clade and most closely related to the subfamily

330 Prioninae rather than the remaining Cerambycinae, consistent with the morphological and

331 molecular analyses in previous reports (*Liu et al., 2018*).

332 The results from the BI trees of the nucleotide dataset showed that Lepturinae cluster with

333 the clade (Cerambycinae + Prioninae) with a high support value (Fig. 3). However, in the ML

334 tree, a close relationship between Lamiinae and (Cerambycinae + Prioninae) was supported with

335 100% posterior probabilities (Fig. 3). The relationship between Cerambycinae and Prioninae is

336 not currently understood in great detail. Prioninae were traditionally considered basal in

337 Cerambycidae by morphology (*Hatch, 1956; Svacha, Wang & Chen, 1997; Farrell,1998*). In

338 addition, *Hunt et al. (2007)* and *Haddad et al. (2018)* pointed out that Prioninae could be placed

339 at the basal position of Cerambycidae based on molecular phylogenetic studies. However, in BI

340 and ML analyses of the 13P26 dataset Prioninae clustered into Cerambycinae, which was

341 consistent with the phylogenetic position of Prioninae recovered by *Raje, Ferris & Holland*

342 *(2016)*.

343 The most controversial point in our results was in Cerambycinae (Fig. 3), which was

344 represented by five different genera and rendered non-monphyletic in Prioninae. However,

345 Cerambycinae was not supported as monophyletic based on molecular by *Liu et al. (2018)* and

346 *Haddad et al. (2018)*, but was recovered in other molecular studies (*Lim et al., 2017; Liu et al.,*

347 *2017*).

348 To further discuss the monophyly of subfamilies within Cerambycidae, more samples were

349   needed to confirm and rebuild the phylogenetic relationship of Cerambycidae using 12 protein-

350   coding genes. The phylogenetic relationships were reconstructed based on the nucleotide data

351   (12P38) with BI and ML methods (Fig. 4). Prioninae still clustered into Cerambycinae in BI and

352   ML analyses of the 12P38 dataset, which agreed with the phylogenetic position of Prioninae

353   recovered using the 13P26 dataset. In BI and ML analyses, all trees recovered the monophyly of

354   Lamiinae (although the relationships within Lamiinae were different). The Lamiinae formed a

355   sister group to a clade comprising Disteniidae, Prioninae, Cerambycinae and Vesperidae. The

356   clade of Lepturinae and Necydalinae was a sister to the remaining species of Cerambycidae *s. l.*.

357   In addition, BI and ML analyses recovered the monophyly of Prioninae including *Callipogon*

358   *relictus*, *Dorysthenes paradoxus* and *Aegosoma sinicum*, as proposed by *Wang et al. (2019)*.

359   However, BI and ML results did not support the monophyly of Cerambycinae with respect to

360   Prioninae and *Spiniphilus spinicornis* (Vesperidae). It has been well accepted that Necydalinae

361   and Lepturinae have a close relationship. The monophyly of Lepturinae was recovered in both BI

362   and ML analyses of the 13P26 dataset. However, BI and ML trees from the 12P38 dataset

363   returned a paraphyletic Lepturinae, due to a sister relationship between *Necydalis ulmi*

364   (Necydalinae) and *Brachyta interrogationis* (Fig. 4).

365   Previous studies recognized *S. spinicornis* as a species of Vesperinae in Cerambycidae

366   (*Napp, 1994*). Nevertheless, subsequent studies considered it to belong to the subfamily Philinae

367   of Vesperidae (*Svacha, Wang & Chen, 1997; Lin & Bi, 2011; Nie et al., 2017*). Further

368   phylogenetic studies put *S. spinicornis* in the fairly controversial placements (*Bi & Lin, 2015;*

369   *Liu et al., 2018*). In addition to our results, a recent molecular study also indicated a similar

370   relationship (*Liu et al., 2018*).

CONCLUSION

372   In this study, we present five completely sequenced mitogenomes of Cerambycidae. The

373   five longicorn beetle species shared similar gene organization with the insects previously

374   reported. The gene sequences and composition of the mitogenomes were relatively conservative

375   with no rearrangements, duplications or deletions. Two large intergenic spacers existed in

376   *Pterolophia* sp. ZJY-2019. The duplication/random loss model and slipped-strand mispairing

377   may explain the existence of these regions. The phylogenetic results inferred from mitogenomes

378   supported the monophyly of Lamiinae and Prioninae in BI and ML analyses, whereas the

379   Cerambycinae and Lepturinae were recovered as non-monophyletic. Although data collected

380   thus far could not resolve the phylogenetic relationships within Cerambycidae, this study will

381   increase the richness of the Cerambycidae genome information and assist in phylogenetic,

382   molecular systematics and evolutionary studies of Cerambycidae.

384   **References**

385   Amaral DT, Mitani Y, Ohmiya Y, Viviani VR. 2016. Organization and comparative analysis of the mitochondrial
386   genomes of *Bioluminescent Elateroidea* (Coleoptera: Polyphaga). Gene 586(2):254-262. DOI
387   10.1016/j.gene.2016.04.009.

388   Anderson S, Bankier AT, Barrell BG, Bruijin MHL, Droujn ARJ, Eperon IC, Nierlich DP, Roe BA, Sanger F,
389   Schreier PH. 1981. Sequence and organization of the human mitochondrial genome. Nature 290(5806):457-465.
390   DOI 10.1038/290457a0.

391   Andrews RM, Kubacka I, Chinnery PF. 1999. Reanalysis and revision of the Cambridge reference sequence for
392   human mitochondrial DNA. Nature Genetics 23(2):147. DOI 10.1038/13779.

393   Avise JC, Arnold J, Ball RM, Bermingham E, Lamb T, Neigel JE, Reeb CA, Saunders NC. 1987. Intraspecific
394   phylogeography: the mitochondrial DNA bridge between population genetics and systematics. Annual Review
395   of Ecology and Systematics 18(1):489–522. DOI 10.1146/annurev.es.18.110187.002421.

396   Bae JS, Kim I, Sohn HD, Jin BR. 2004. The mitochondrial genome of the firefly, *Pyrocoelia rufa*: complete DNA
397   sequence, genome organization, and phylogenetic analysis with other insects. Molecular Phylogenetics and
398   Evolution 32(3):978-985. DOI 10.1016/j.ympev.2004.03.009.

399   Benson G. 1999. Tandem repeats finder: a program to analyze DNA sequences. Nucleic Acids Research 27(2):573-
400   580. DOI 10.1093/nar/27.2.573.

401   Bernt M, Donath A, Jühling F, Externbrink F, Florentz C, Fritzsch G, Pütz J, Middendorf M, Stadler PF. 2013.
402   MITOS: improved de novo metazoan mitochondrial genome annotation. Molecular Phylogenetics and
403   Evolution 69(2):313–319. DOI 10.1016/j.ympev.2012.08.023.

404   Bi W, Lin M. 2015. Discovery of second new species of the genus *Spiniphilus* Lin & Bi, and female of *Heterophilus*
405   *scabricollis* Pu with its biological notes (Coleoptera: Vesperidae: Philinae: Philini). Zootaxa. 3949(4):575-583.
406   DOI 10.11646/zootaxa.3949.4.7.

407   Bologna MA, Oliverio M, Pitzalis M, Mariottini P. 2008. Phylogeny and evolutionary history of the blister beetles
408   (Coleoptera,   Meloidae).   Molecular   Phylogenetics   and   Evolution   48(2):679-693.   DOI
409   10.1016/j.ympev.2008.04.019.

410   Boore JL, Lavrov DV, BrownWM. 1998. Gene translocation links insects and crustaceans. Nature 392(6677):667–
411   668. DOI 10.1038/33577.

412   Boore JL. 1999. Animal mitochondrial genomes. Nucleic Acids Research 27(8):1767–1780. DOI
413   10.1093/nar/27.8.1767.

414   Boore JL, Brown WM. 2000. Mitochondrial genomes of *Galathealinum*, *Helobdella*, and *Platynereis*: sequence and
415   gene arrangement comparisons indicate that Pogonophora is not a Phylum and Annelida and Arthropoda are
416   not sister taxa. Molecular Biology and Evolution 17(1):87-106.
417   DOI10.1093/oxfordjournals.molbev.a026241.

418   Boore JL. 2001. Complete mitochondrial genome sequence of the polychaete annelid *Platynereis dumerilii*.
419   Molecular Biology and Evolution 18(7):1413-1416. DOI 10.1186/1471-2164-5-67.

420   Burland TG. 2000. DNASTAR's Lasergene sequence analysis software. In: Misener S, Krawetz SA, eds.
421   Bioinformatics Methods and Protocols. Methods in Molecular Biology. Totowa: Humana Press, 71–91.

422   Cameron SL. 2014. How to sequence and annotate insect mitochondrial genomes for systematic and comparative
423   genomics research. Systematic Entomology 39(3):400–411. DOI 10.1111/syen.12071.

424   Castresana J. 2000. Selection of conserved blocks from multiple alignments for their use in phylogenetic analysis.

425   Molecular Biology and Evolution 17(4):540–552. DOI 10.1093/oxfordjournals.molbev.a026334.

426 Chai HN, Du YZ. 2012. The complete mitochondrial genome of the pink stem borer, *Sesamia inferens*, in

427   comparison with four other noctuid moths. International Journal of Molecular Sciences 13(8):10236-10256.

428   DOI 10.3390/ijms130810236.

429 Cheng XF, Zhang LP, Yu DN, Storey KB, Zhang JY. 2016. The complete mitochondrial genomes of four

430   cockroaches (Insecta: Blattodea) and phylogenetic analyses within cockroaches. Gene 586:115-122. DOI

431   10.1016/j.gene.2016.03.057.

432 Chiu WC, Yeh WB, Chen ME, Yang MM. 2016. Complete mitochondrial genome of *Aeolesthes oenochrous*

433   (Fairmaire) (Coleoptera: Cerambycidae): an endangered and colorful longhorn beetle. Mitochondrial DNA Part

434   A. 27(1):686–687. DOI 10.3109/19401736.2014.913143.

435 Coates, Brad S. 2014. Assembly and annotation of full mitochondrial genomes for the corn rootworm species,

436   *Diabrotica virgifera virgifera* and *Diabrotica barberi* (Insecta: Coleoptera: Chrysomelidae), using next

437   generation sequence data. Gene 542(2):190-197. DOI 10.1016/j.gene.2014.03.035.

438 Dotson EM, Beard CB. 2001. Sequence and organization of the mitochondrial genome of the Chagas disease vector,

439   *Triatoma dimidiata*. Insect Molecular Biology 10(3):205-215. DOI 10.1046/j.1365-2583.2001.00258.x.

440 Du C, He SL, Song XH, Liao Q, Zhang XY, Yue BS. 2016. The complete mitochondrial genome of *Epicauta*

441   *chinensis* (Coleoptera: Meloidae) and phylogenetic analysis among coleopteran insects. Gene 578(1):274–280.

442   DOI 10.1016/j.gene.2015.12.036.

443 Du C, Zhang LF, Lu T, Ma JN, Zeng CJ, Yue BS, Zhang XY. 2017. Mitochondrial genomes of blister beetles

444   (Coleoptera, Meloidae) and two large intergenic spacers in *Hycleus* genera. BMC Genomics 18(1):698. DOI

445   10.1186/s12864-017-4102-y.

446 Eyrewaker A. 1997. Differentiating between selection and mutation bias. Genetics 147(4):1983-1987.

447 Fang J, Qian L, Xu M, Yang X, Wang B, An Y. 2016. The complete nucleotide sequence of the mitochondrial

448   genome of the Asian longhorn beetle, *Anoplophora glabripennis* (Coleoptera: Cerambycidae). Mitochondrial

449   DNA Part A 27(5):3299-3300. DOI 10.3109/19401736.2015.1015012.

450 Farrell BD. 1998. "Inordinate fondness" explained: Why are there so many beetles? Science 281(5376):555-559.

451   DOI 10.1126/science.281.5376.555.

452 Foster PG, Jermiin LS, Hickey DA. 1997. Nucleotide composition bias affects amino acid content in proteins coded

453   by animal mitochondria. Journal of Molecular Evolution 44(3):282-288. DOI 10.1007/pl00006145.

454 Friedrich M, Muqim N. 2003. Sequence and phylogenetic analysis of the complete mitochondrial genome of the

455   flour beetle *Tribolium castanaeum*. Molecular Phylogenetics and Evolution 26(3):502-512. DOI

456   10.1016/s1055-7903(02)00335-4.

457 Gao XY, Cai YY, Yu DN, Storey KB, Zhang JY. 2018. Characteristics of the complete mitochondrial genome of

458   *Suhpalacsa longialata* (Neuroptera, Ascalaphidae) and its phylogenetic implications. PeerJ 6:e5914. DOI

459   10.7717/peerj.5914.

460 Gong R, Guo X, Ma J, Song X, Shen Y, Geng F, Yue B. 2018. Complete mitochondrial genome of *Periplaneta*

461   *brunnea* (Blattodea: Blattidae) and phylogenetic analyses within Blattodea. Journal of Asia-Pacific Entomology

462   21(3): 885-895. DOI 10.1016/j.aspen.2018.05.006.

463 Grant JR, Stothard P. 2008. The CG View Server: a comparative genomics tool for circular genomes. Nucleic Acids

464   Research 36(2):181-184. DOI 10.1093/nar/gkn179.

465 Guo K, Chen J, Xu CQ, Qiao HL, Xu R, Zhao XJ. 2016. The complete mitochondrial genome of the longhorn beetle

466   *Xylotrechus grayii* (Coleoptera: Cerambycidae). Mitochondrial DNA Part A 27(3):2133-2134. DOI
467   10.3109/19401736.2014.982592.

468   Haddad S, Shin S, Lemmon AR, Lemmon EM, Svacha P, Farrell B, McKenna DD. 2018. Anchored hybrid
469   enrichment provides new insights into the phylogeny and evolution of longhorned beetles (Cerambycidae).
470   Systematic Entomology 43(1):68-89. DOI 10.1111/syen.12257.

471   Hanada T, Suzuki T, Yokogawa T, Takemoto-Hori C, Sprinzl M, Watanabe K. 2001. Translation ability of
472   mitochondrial tRNAs[Ser] with unusual secondary structures *in an in vitro* translation system of bovine
473   mitochondria. Genes to Cells 6(12):1019–1030. DOI 10.1046/j.1365-2443.2001.00491.x.

474   Hatch MH. 1956. The natural classification of the families of Coleoptera. Annals of the Entomological Society of
475   America 49(1):102. DOI 10.1093/aesa/49.1.102.

476   Hua J, Li M, Dong P, Cui Y, Xie Q, Bu W. 2008. Comparative and phylogenomic studies on the mitochondrial
477   genomes of *Pentatomomorpha* (Insecta: Hemiptera: Heteroptera). BMC Genomics 9(1): 610. DOI
478   10.1186/1471-2164-9-610.

479   Hunt T, Bergsten J, Levkanicova Z, Papadopoulou A, John OS, Wild R, Gómez-Zurita J. 2007. A comprehensive
480   phylogeny of beetles reveals the evolutionary origins of a superradiation. Science 318(5858):1913-1916. DOI
481   10.1126/science.1146954.

482   Kim KG, Hong MY, Kim MJ, Im HH, Kim MI, Bae CH. 2009. Complete mitochondrial genome sequence of the
483   yellow-spotted long-horned beetle *Psacothea hilaris* (Coleoptera: Cerambycidae) and phylogenetic analysis
484   among coleopteran insects. Molecules and Cells 27(4):429-441. DOI 10.1007/s10059-009-0064-5.

485   Kim S, de Medeiros BA, Byun BK, Lee S, Kang JH, Lee B, Farrell BD. 2018. West meets East: How do rainforest
486   beetles become circum-Pacific? Evolutionary origin of *Callipogon relictus* and allied species (Cerambycidae:
487   Prioninae) in the new and old worlds. Molecular Phylogenetics and Evolution, 125:163-176. DOI
488   10.1016/j.ympev.2018.02.019.

489   Kumar S, Stecher G, Tamura K. 2016. Mega 7: molecular evolutionary genetics analysis version 7.0 for bigger
490   datasets. Molecular Biology and Evolution 33(7):1870–1874. DOI 10.1093/molbev/msw054.

491   Lanfear R, Calcott B, Ho SYW, Guindon S. 2012. PartitionFinder: combined selection of partitioning schemes and
492   substitution models for phylogenetic analyses. Molecular Biology and Evolution 29(6):1695–1701. DOI
493   10.1093/molbev/mss020.

494   Lawrence JF, Newton AF. 1982. Evolution and classification of beetles. Annual Review of Ecology and Systematics
495   13(1):261–290. DOI 10.1146/annurev.es.13.110182.001401.

496   Levinson G, Gutman GA. 1987. Slipped-strand mispairing: a major mechanism for DNA sequence evolution.
497   Molecular Biology and Evolution 4(3):203–221. DOI 10.1093/oxfordjournals.molbev.a040442.

498   Li F, Zhang H, Wang W, Weng H, Meng Z. 2016a. Complete mitochondrial genome of the Japanese pine sawyer,
499   *Monochamus alternatus* (Coleoptera: Cerambycidae). Mitochondrial DNA Part A 27(2):1144-1145. DOI
500   10.3109/19401736.2014.936321.

501   Li W, Yang X, Qian L, An Y, Fang J. 2016b. The complete mitochondrial genome of the citrus long-horned beetle,
502   *Anoplophora chinensis* (Coleoptera: Cerambycidae). Mitochondrial DNA Part A 27(6): 4665–4667. DOI
503   10.3109/19401736.2015.1106493.

504   Lim J, Yi DK, Kim YH, Lee W, Kim S, Kang JH. 2017. Complete mitochondrial genome of *Callipogon relictus*
505   Semenov (Coleoptera: Cerambycidae): a natural monument and endangered species in Korea. Mitochondrial
506   DNA Part B 2(2):629-631. DOI 10.1080/23802359.2017.1372718.

507 Lin M, Bi W. 2011. A new genus and species of the subfamily Philinae (Coleoptera: Vesperidae). Zootaxa
508   2777(1):54-60. DOI 10.11646/zootaxa.2777.1.4.

509 Liu JH, Jia PF, Luo T, Wang QM. 2017. Complete mitochondrial genome of white-striped long-horned beetle,
510   *Batocera lineolata* (Coleoptera: Cerambycidae) by next-generation sequencing and its phylogenetic
511   relationship within superfamily Chrysomeloidea. Mitochondrial DNA Part B 2(2):520-521. DOI
512   10.1080/23802359.2017.1361797.

513 Liu YQ, Chen DB, Liu HH, Hu HL, Bian HX, Zhang RS. 2018. The complete mitochondrial genome of the
514   longhorn beetle *Dorysthenes Paradoxus* (Coleoptera: Cerambycidae: Prionini) and the implication for the
515   phylogenetic relationships of the Cerambycidae species. Journal of Insect Science 18(2). DOI
516   10.1093/jisesa/iey012.

517 Ma Y, He K, Yu PP, Cheng XF, Zhang JY. 2015. The complete mitochondrial genomes of three bristletails (Insecta:
518   Archaeognatha): the paraphyly of Machilidae and insights into Archaeognathan phylogeny. PLOS ONE
519   10:e0117669. DOI 10.1371/journal.pone.0117669.

520 Ma ZH, Yang XF, Bercsenyi M, Wu JJ, Yu Y, Wei K, Qi XF, Yang RB. 2015. Comparative mitogenomics of the
521   genus *Odontobutis* (Perciformes: Gobioidei: Odontobutidae) revealed conserved gene rearrangement and high
522   sequence   variations.   International   Journal   of   Molecular   Sciences   16(10):25031-25049.   DOI
523   10.3390/ijms161025031.

524 Min XJ, Hickey DA. 2007. DNA asymmetric strand bias affects the amino acid composition of mitochondrial
525   proteins. DNA Research 14(5):201-206. DOI 10.1093/dnares/dsm019.

526 Monné ML, Monné MA, Mermudes JRM. 2009. Inventário das espécies de Cerambycinae (Insecta, Coleoptera,
527   Cerambycidae) do Parque Nacional do Itatiaia, RJ, Brasil. Biota Neotropica 12(12):40-76. DOI 10.1590/S1676-
528   06032012000100004.

529 Moritz C, Dowling TE, Brown WM. 1987. Evolution of animal mitochondrial DNA: relevance for population
530   biology and systematics. Annual Review of Ecology and Systematics 18(1):269-292. DOI 10.2307/2097133.

531 Napp DS. 1994. Phylogenetic relationships among the subfamilies of Cerambycidae (Coleoptera, Chrysomeloidea).
532   Revista Brasileira de Entomologia 38(2):265-419.

533 Negrisolo E, Babbucci M, Patarnello T. 2011. The mitochondrial genome of the ascalaphid owlfly *Libelloides*
534   *macaronius*, and comparative evolutionary mitochondriomics of neuropterid insects. BMC Genomics
535   12(1):221. DOI 10.1186/1471-2164-12-221.

536 Nie R, Lin M, Xue H, Bai M, Yang X. 2017. Complete mitochondrial genome of *Spiniphilus spinicornis*
537   (Coleoptera: Vesperidae: Philinae) and phylogenetic analysis among Cerambycoidea. Mitochondrial DNA Part
538   A 28(1):145-146. DOI 10.3109/19401736.2015.1111363.

539 Ojala D, Montoya J, Attardi G. 1981. tRNA punctuation model of RNA processing in human mitochondria. Nature
540   290(5806):470–474. DOI 10.1038/290470a0.

541 Perna NT, Kocher TD. 1995. Patterns of nucleotide composition at fourfold degenerate sites of animal
542   mitochondrial genomes. Journal of Molecular Evolution 41(3):353–358. DOI 10.1007/bf01215182.

543 Ponomarenko AG, Prokin AA. 2015. Review of paleontological data on the evolution of aquatic beetles
544   (Coleoptera). Paleontological Journal 49(13):1383-1412. DOI 10.1134/S0031030115130080.

545 Powell JR, Moriyama EN. 1997. Evolution of codon usage bias in drosophila. Proceedings of the National Academy
546   of Sciences 94(15):7784-7790. DOI 10.2307/2097133.

547 Que S, Yu A, Liu P, Jin M, Xie GA. 2019. The complete mitochondrial genome of *Apriona swainsoni*.

548   Mitochondrial DNA Part B 4(1):931-932. DOI 10.1080/23802359.2019.1567284.

549   Raje KR, Ferris VR, Holland JD. 2016. Phylogenetic signal and potential for invasiveness. Agricultural and Forest
550   Entomology 18(3):260-269. DOI 10.1111/afe.12158.

551   Rao Y, Wu G, Wang Z, Chai X, Nie Q, Zhang X. 2011. Mutation bias is the driving force of codon usage in the
552   *Gallus gallus* genome. DNA Research 18(6):499-512. DOI 10.1093/dnares/dsr035.

553   Reid CAM. 1995. A cladistic analysis of subfamilial relationships in the Chrysomelidae *s. l.* (Chrysomeloidea).
554   Biology, Phylogeny and Classification of Coleoptera: Papers Celebrating the 80th Birthday of Roy A. Crowson
555   559-631.

556   Rodovalho CM, Lyra ML, Ferro M, Jr MB. 2014. The mitochondrial genome of the leaf-cutter ant *Atta laevigata*: a
557   mitogenome with a large number of intergenic spacers. PLoS ONE 9(5): e97117. DOI
558   10.1371/journal.pone.0097117.

559   Ronquist F, Teslenko M, Mark PVD, Ayres DL, Darling A, Höhna S, Larget B, Liu L, Suchard MA, Huelsenbeck
560   JP. 2012. MrBayes 3.2: efficient Bayesian phylogenetic inference and model choice across a large model space.
561   Systematic Biology 61(3):539–542. DOI 10.1093/sysbio/sys029.

562   Saito S, Tamura K, Aotsuka T. 2005. Replication origin of mitochondrial DNA in insects. Genetics 171(4):1695-
563   1705. DOI 10.1534/genetics.105.046243.

564   Sama G, Buse J, Orbach E, Friedman A, Rittner O, Chikatunov V. 2010. A new catalogue of the Cerambycidae
565   (Coleoptera) of Israel with notes on their distribution and host plants. Munis Entomology and Zoology 5(1):1–
566   55. DOI 10.1007/s12032-010-9513-4.

567   Sheffield NC, Song H, Cameron SL, Whiting MF. 2008. A comparative analysis of mitochondrial genomes in
568   Coleoptera (Arthropoda: Insecta) and genome descriptions of five new beetles. Molecular Biology and
569   Evolution 25(11):2499–2509. DOI 10.1093/molbev/msn198.

570   Simon C, Buckley TR, Frati F, Stewart JB, Beckenbach AT. 2006. Incorporating molecular evolution into
571   phylogenetic analysis, and a new compilation of conserved polymerase chain reaction primers for animal
572   mitochondrial DNA. Annual Review of Ecology Evolution and Systematics 37(1):545–579. DOI
573   10.1146/annurev.ecolsys.37.091305.110018.

574   Song H, Sheffield NC, Cameron SL, Miller KB, Whiting MF. 2010. When phylogenetic assumptions are violated:
575   base compositional heterogeneity and among-site rate variation in beetle mitochondrial phylogenomics.
576   Systematic Entomology 35(3):429-448. DOI 10.1111/j.1365-3113.2009.00517.x.

577   Song N, Zhang H, Yin X, Lin A, Zhai Q. 2017. The complete mitochondrial genome sequence from the longicorn
578   beetle *Obrium* sp. (Coleoptera: Cerambycidae). Mitochondrial DNA Part A 28(3):326-327. DOI
579   10.3109/19401736.2015.1122766.

580   Stamatakis A. 2014. RAxML version 8: a tool for phylogenetic analysis and post-analysis of large phylogenies.
581   Bioinformatics 30(9):1312–1313. DOI 10.1093/bioinformatics/btu033.

582   Steinberg S, Cedergren R. 1994. Structural compensation in atypical mitochondrial tRNAs. Nature Structural
583   Biology 1(8):507–510. DOI 10.1038/nsb0894-507.

584   Stewart JB, Beckenbach AT. 2003. Phylogenetic and genomic analysis of the complete mitochondrial DNA
585   sequence of the spotted asparagus beetle *Crioceris duodecimpunctata*. Molecular Phylogenetics and Evolution
586   26(3):513–526. DOI 10.1016/S1055-7903(02)00421-9.

587   Svacha P, Wang J, Chen S. 1997. Larval morphology and biology of *Philus antennatus* and *Heterophilus*
588   *punctulatus*, and systematic position of the Philinae (Coleoptera: Cerambycidae: Vesperidae). Annales de la

589   Société Entomologique de France 33:323-369.

590   Taanman JW. 1999. The mitochondrial genome: structure, transcription, translation and replication. Biophysica Acta

591   (BBA)-Bioenergetics 1410(2):103-123. DOI 10.1016/S0005-2728(98)00161-3.

592   Tan MH, Gan HM, Lee YP, Poore GC, Austin CM. 2017. Digging deeper: new gene order rearrangements and

593   distinct patterns of codons usage in mitochondrial genomes among shrimps from the Axiidea, Gebiidea and

594   Caridea (Crustacea: Decapoda). PeerJ 5:e2982. DOI 10.7717/peerj.2982.

595   Timmermans, Martijn JTN, Vogler AP. 2012. Phylogenetically informative rearrangements in mitochondrial

596   genomes of Coleoptera, and monophyly of aquatic elateriform beetles (Dryopoidea). Molecular Phylogenetics

597   and Evolution 63(2):299-304. DOI 10.1016/j.ympev.2011.12.021

598   Wang J, Lan DY, Dai XY, Yu DN, Storey KB, Zhang JY. 2019. The complete mitochondrial genome of *Xystrocera*

599   *globosa* (Coleoptera: Cerambycidae) and its phylogeny. Mitochondrial DNA Part B 4(1):1647-1649. DOI:

600   10.1080/23802359.2019.1605852.

601   Wang Q, Tang G. 2017. Genomic and phylogenetic analysis of the complete mitochondrial DNA sequence of

602   walnut leaf pest *Paleosepharia posticata* (Coleoptera: Chrysomeloidea). Journal of Asia-Pacific Entomology

603   20(3): 840-853. DOI 10.1016/j.aspen.2017.05.010.

604   Wang YT, Liu YX, Tong XL, Ren QP, Jiang GF. 2016. The complete mitochondrial genome of the longhorn beetle,

605   *Massicus raddei*. Mitochondrial DNA Part A 27(1):209-211 DOI 10.3109/19401736.2014.880892.

606   Wei SJ, Tang P, Zheng LH, Shi M, Chen XX. 2010. The complete mitochondrial genome of *Evania appendigaster*

607   (Hymenoptera: Evaniidae) has low A+ T content and a long intergenic spacer between atp8 and atp6.

608   Molecular Biology Reports 37(4): 1931-1942. DOI 10.1007/s11033-009-9640-1.

609   Wolstenholme DR. 1992. Animal mitochondrial DNA: structure and evolution. International Review of Cytology

610   141:173–216. DOI 10.1016/S0074-7696(08)62066-5.

611   Yuan M, Zhang Q, Zhang L, Guo Z, Liu Y, Shen Y. 2016. High-level phylogeny of the Coleoptera inferred with

612   mitochondrial genome sequences. Molecular Phylogenetics and Evolution 104:99-111. DOI

613   10.1016/j.ympev.2016.08.002.

614   Yukuhiro K, Sezutsu H, Itoh M, Shimizu K, Banno Y. 2002. Significant levels of sequence divergence and gene

615   rearrangements have occurred between the mitochondrial genomes of the wild mulberry silkmoth, *Bombyx*

616   *mandarina*, and its close relative, the domesticated silkmoth, *Bombyx mori*. Molecular Biology and Evolution

617   19(8):1385-1389. DOI 10.1093/oxfordjournals.molbev.a004200.

618   Zhang JY, Zhou CF, Gai YH, Song DX, Zhou KY. 2008. The complete mitochondrial genome of *Parafronurus youi*

619   (Insecta: Ephemeroptera) and phylogenetic position of the Ephemeroptera. Gene 424(1–2):18-24. DOI

620   10.1016/j.gene.2008.07.037.

621   Zhang DX, Hewitt GM. 1997. Insect mitochondrial control region: A review of its structure, evolution and

622   usefulness in evolutionary studies. Biochemical Systematics and Ecology 25(2):99-120. DOI 10.1016/s0305-

623   1978(96)00042-7.

624   Zhang LP, Cai YY, Yu DN. Storey KB, Zhang JY. 2018a. Gene characteristics of the complete mitochondrial

625   genomes of *Paratoxodera polyacantha* and *Toxodera hauseri* (Mantodea: Toxoderidae). PeerJ 6:e4595. DOI

626   10.7717/peerj.4595.

627   Zhang LP, Ma Y, Yu DN, Storey KB, Zhang JY. 2019. The mitochondrial genomes of *Statilia maculata* and *S.*

628   *nemoralis* (Mantidae: Mantinae) with different duplications of *trnR* genes. International Journal of Biological

629   Macromolecules 121:839-845. DOI 10.1016/j.ijbiomac.2018.10.038.

630   Zhang LP, Yu DN, Storey KB, Cheng HY, Zhang JY. 2018b. Higher tRNA gene duplication in mitogenomes of
631   praying mantises (Dictyoptera, Mantodea) and the phylogeny within Mantodea. International Journal of
632   Biological Macromolecules 111:787-795. DOI 10.1016/j.ijbiomac.2018.01.016.
633   Zhang SQ, Che LH, Li Y, Liang D, Pang H, Ślipiński A, Zhang P. 2018c. Evolutionary history of Coleoptera
634   revealed by extensive sampling of genes and species. Nature Communications 9(1):205. DOI 10.1038/s41467-
635   017-02644-4.

637 **Ethics Approval and Consent to Participate**

638 All the samples of longicorn beetles were permitted under the scientific research in China.

639 **Competing interests**

640 The authors declare that they have no competing interests.

641 **Acknowledgments**

642 We are grateful to Wen-Yong Feng for his help in sample collection.

643 **Funding**

644 This research was supported by the Zhejiang provincial Natural Science Foundation (Y18C040006), the

645 National Natural Science Foundation of China (31370042), the College students' Innovation and

646 Entrepreneurship Project in China (No. 201810345043), the College students in Zhejiang Normal University

647 Innovation and Entrepreneurship Plan (2018-317) for the study design, data collection and analyses.

648 **Author Contributions**

649 Conceived and designed the experiments: JW XYD DNY JYZ. Performed the experiments: JW XYD.

650 Analyzed the data: JW XYD XDX ZYZ DNY JYZ. Contributed reagents/materials/analysis tools: JW XYD

651 JYZ DNY. Wrote the paper: JW XYD XDX ZYZ DNY KBS JYZ. All the authors read and approved the final

652 version of the manuscript.

653 **ORCID**

654 Jia-Yong Zhang   http://orcid.org/0000-0002-7679-2548

655 Dan-Na Yu   http://orcid.org/0000-0002-9870-1926

656 Kenneth B. Storey   http://orcid.org/000-0002-7363-1853

657 Jun Wang   https://orcid.org/0000-0003-1520-8691

658 XY Dai   https://orcid.org/0000-0001-6832-1546

659 XD Xu   https://orcid.org/0000-0002-3682-9967

660 ZY Zhang https://orcid.org/0000-0001-8159-9104

662 **Figure legends**

663 **Figure 1 The RSCU of five longicorn beetle mitochondrial genomes.** Codon families are provided on the x-axis along with the

664 different combinations of synonymous codons that code for that amino acid. RSCU (relative synonymous codon usage) is defined

665 on the Y axis.

666 **Figure 2 Putative mechanisms for formation of the two large intergenic regions (IGRs) that exist in *Pterolophia* sp. ZJY-**

667 **2019. (**a) The slipped-strand mispairing and random loss model to explain the 157 bp-IGR between *trnS2* and *nad1*. The CS

668 indicates the 18 bp conservative sequence TTACTAAATTTAATTAACTAAA. (b) The duplication/random loss model to

669 explain the 184 bp-IGR between *trnC* and *trnY*.

670 **Figure 3 Phylogenetic relationships of Cerambycidae in BI and ML analyses.** The data includes 23 species of Cerambycidae

671 as the ingroup and three species of Chrysomelidae as the outgroup. The GenBank accession numbers of all species are also

672 shown.

673 **Figure 4 Phylogenetic relationships of Cerambycidae in BI and ML analyses.** The data includes 35 species of Cerambycidae

674 as the ingroup and three species of Chrysomelidae as the outgroup. The GenBank accession numbers of all species are also

675 shown.

676 **Figure S1 Mitochondrial genome maps of *O. yaoshana*.** The first circle shows the gene map (PCGs, rRNAs, tRNAs and the

677 AT-rich region) and the genes outside the map are coded on the majority strand (J-strand) whereas the genes inside the map are

678 coded on the minority strand (N-strand). The second circle shows the GC content and the third shows the GC skew. Both GC

679 content and GC skew are plotted as the deviation from the average value of the total sequence.

680 **Figure S2 Mitochondrial genome maps of *T. croccocincta*.** The first circle shows the gene map (PCGs, rRNAs, tRNAs and the

681 AT-rich region) and the genes outside the map are coded on the majority strand (J-strand) whereas the genes inside the map are

682 coded on the minority strand (N-strand). The second circle shows the GC content and the third shows the GC skew. Both GC

683 content and GC skew are plotted as the deviation from the average value of the total sequence.

684 **Figure S3 Mitochondrial genome maps of *B. succinctor*.** The first circle shows the gene map (PCGs, rRNAs, tRNAs and the

685 AT-rich region) and the genes outside the map are coded on the majority strand (J-strand) whereas the genes inside the map are

686 coded on the minority strand (N-strand). The second circle shows the GC content and the third shows the GC skew. Both GC

687 content and GC skew are plotted as the deviation from the average value of the total sequence.

688 **Figure S4 Mitochondrial genome maps of *N. carinicollis*.** The first circle shows the gene map (PCGs, rRNAs, tRNAs and the

689 AT-rich region) and the genes outside the map are coded on the majority strand (J-strand) whereas the genes inside the map are

690 coded on the minority strand (N-strand). The second circle shows the GC content and the third shows the GC skew. Both GC

691 content and GC skew are plotted as the deviation from the average value of the total sequence.

692 **Figure S5 Mitochondrial genome maps of *Pterolophia* sp. ZJY-2019.** The first circle shows the gene map (PCGs, rRNAs,

693 tRNAs and the AT-rich region) and the genes outside the map are coded on the majority strand (J-strand) whereas the genes

694 inside the map are coded on the minority strand (N-strand). The second circle shows the GC content and the third shows the GC

695 skew. Both GC content and GC skew are plotted as the deviation from the average value of the total sequence.

696 **Figure S6 Secondary structure of tRNAs (*trnI-trnV*) in five newly sequenced mitogenomes.**

697 (1): *O. yaoshana* (2): *T. croccocincta* (3): *B. succinctor* (4): *N. carinicollis* (5): *Pterolophia* sp. ZJY-2019

698 A: trnI ; B: trnQ; C: trnM; D: trnW; E: trnC; F: trnY; G: trnL (UUA); H: trnK; I: trnD; J: trnG; K: trnA; L: trnR; M: trnN; N: trnS

699 (AGN); O: trnE; P: trnF; Q: trnH; R: trnT; S: trnP; T: trnS (UCN); U: trn L (CUA); V: trnV.

701 **Table notes**

702 **Table 1** Species used to construct the phylogenetic relationships along with GenBank accession numbers.

703 *Partial genome.

704 **Table 2.** The partition schemes and best-fitting models selected of 13 protein-coding genes in the 13P26

705 dataset.

706 **Table 3.** The partition schemes and best-fitting models selected of 12 protein-coding genes in the 12P38

707 dataset.

708 **Table 4** Base composition of Cerambycidae mitochondrial genomes.

709

710 **Table S1** Universal and specific primers used to amplify the mitochondrial genomes of the five beetle species.

711 **Table S2** Organization of the *O. yaoshana* mitochondrial genome.

712 **Table S3** Organization of the *T. croccocincta* mitochondrial genome.

713 **Table S4** Organization of the *B. succinctor* mitochondrial genome.

714 **Table S5** Organization of the *N. carinicollis* mitochondrial genome.

715 **Table S6** Organization of the *Pterolophia* sp. ZJY-2019 mitochondrial genome.

716 **Table S7.** The codon number and relative synonymous codon usage (RSCU) in mitochondrial protein coding

717 genes.

718

719

Figure 1

Figure 1 The RSCU of five longicorn beetle mitochondrial genomes.

Figure 1 The RSCU of five longicorn beetle mitochondrial genomes. Codon families are provided on the x-axis along with the different combinations of synonymous codons that code for that amino acid. RSCU (relative synonymous codon usage) is defined on the Y axis.
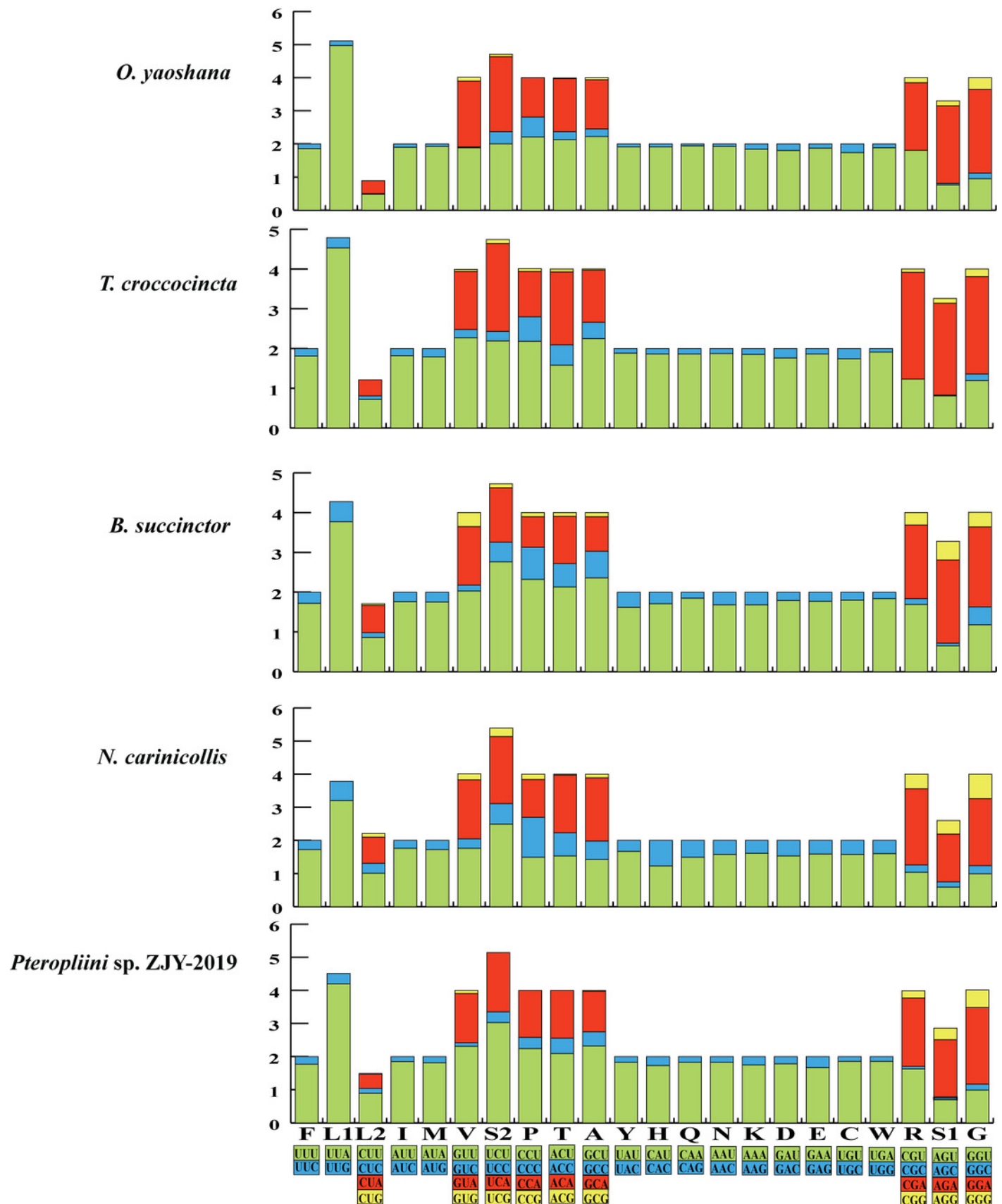
Figure 2

Figure 2 Putative mechanisms for formation of the two large intergenic regions (IGRs) that exist in *Pterolophia* sp. ZJY-2019.

Figure 2 Putative mechanisms for formation of the two large intergenic regions (IGRs) that exist in *Pterolophia* sp. ZJY-2019. (a) The slipped-strand mispairing and random loss model to explain the 157 bp-IGR between *trnS2* and *nad1*. The CS indicates the 18 bp conservative sequence TTACTAAATTTAATTAACTAAA. (b) The duplication/random loss model to explain the 184 bp-IGR between *trnC* and *trnY*.
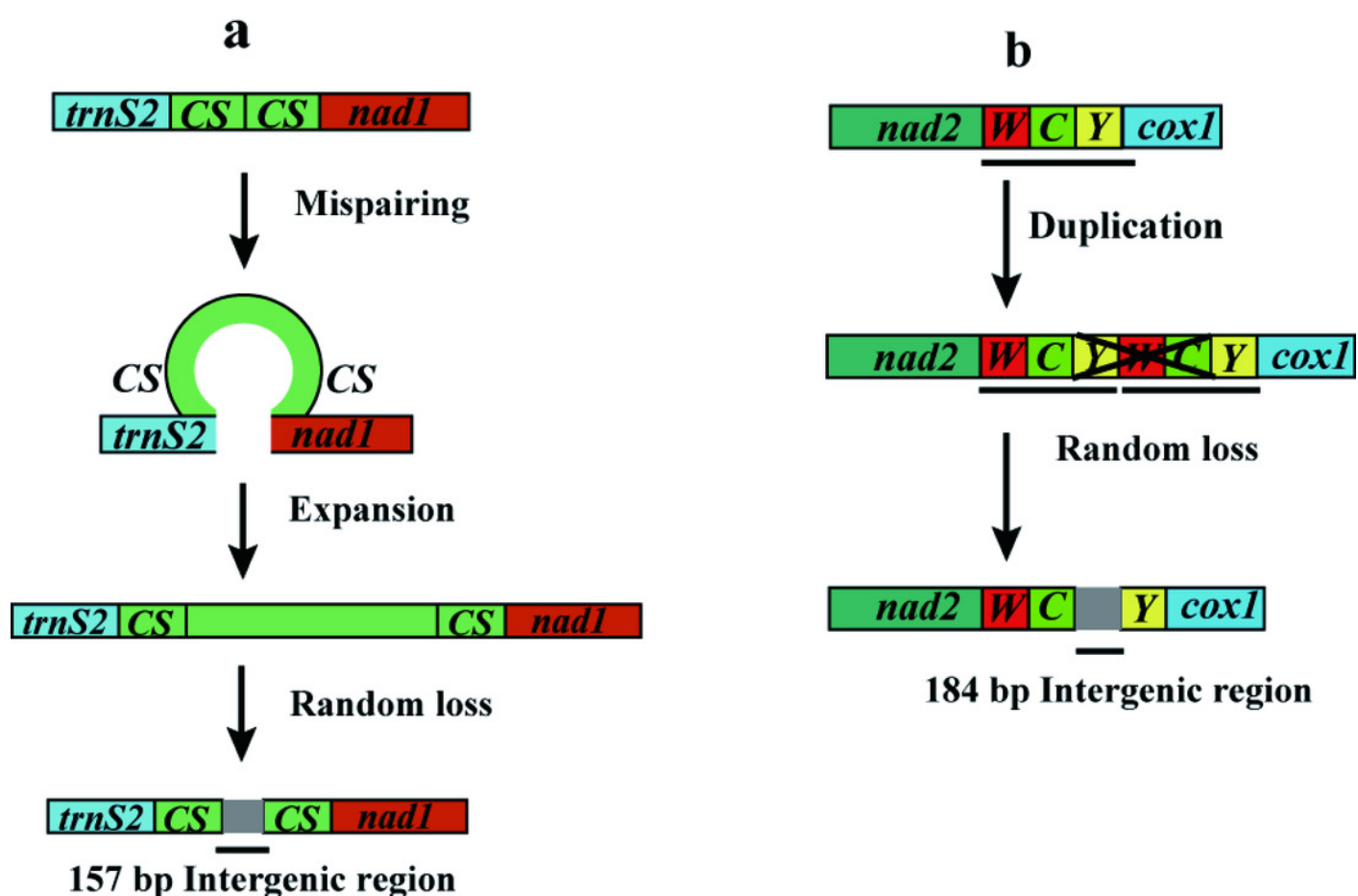
Figure 3

Figure 3 Phylogenetic relationships of Cerambycidae in BI and ML analyses.

Figure 3 Phylogenetic relationships of Cerambycidae in BI and ML analyses. The data includes 23 species of Cerambycidae as the ingroup and three species of Chrysomelidae as the outgroup. The GenBank accession numbers of all species are also shown.
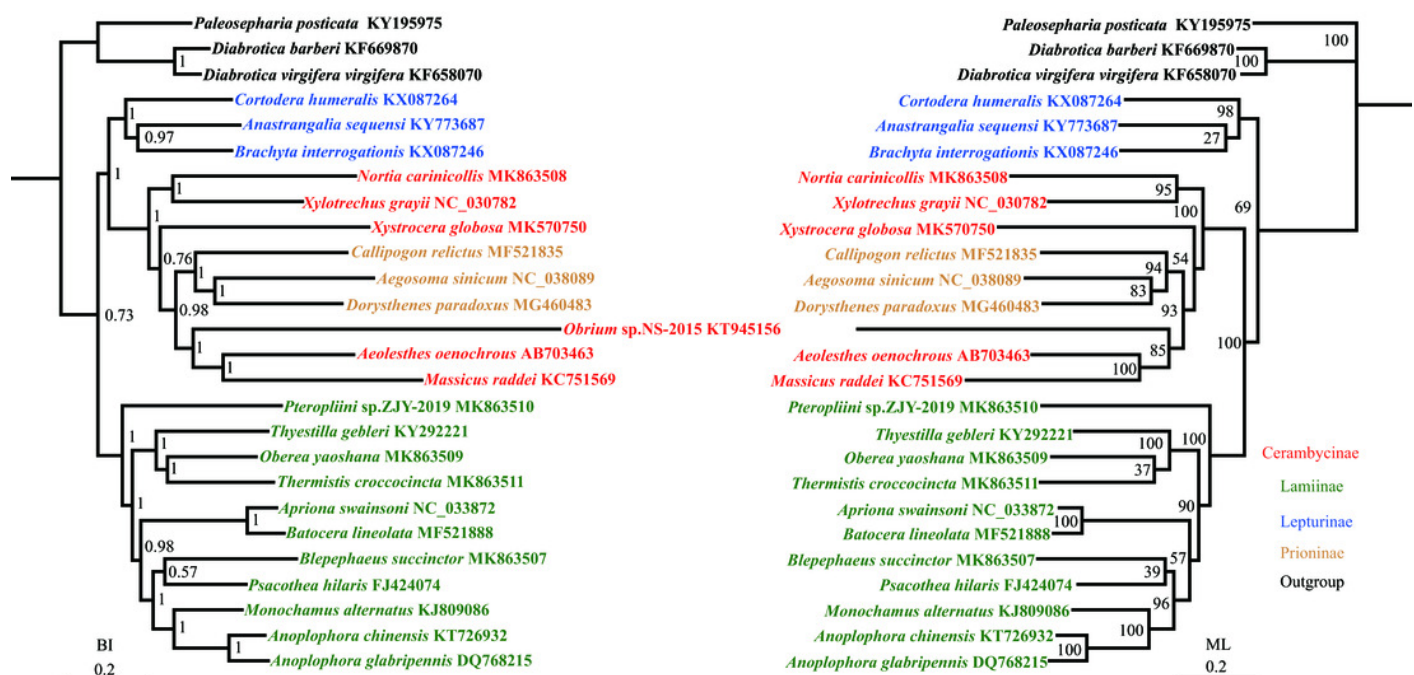
Figure 4

Figure 4 Phylogenetic relationships of Cerambycidae in BI and ML analyses.

Figure 4 Phylogenetic relationships of Cerambycidae in BI and ML analyses. The data includes 35 species of Cerambycidae as the ingroup and three species of Chrysomelidae as the outgroup. The GenBank accession numbers of all species are also shown.
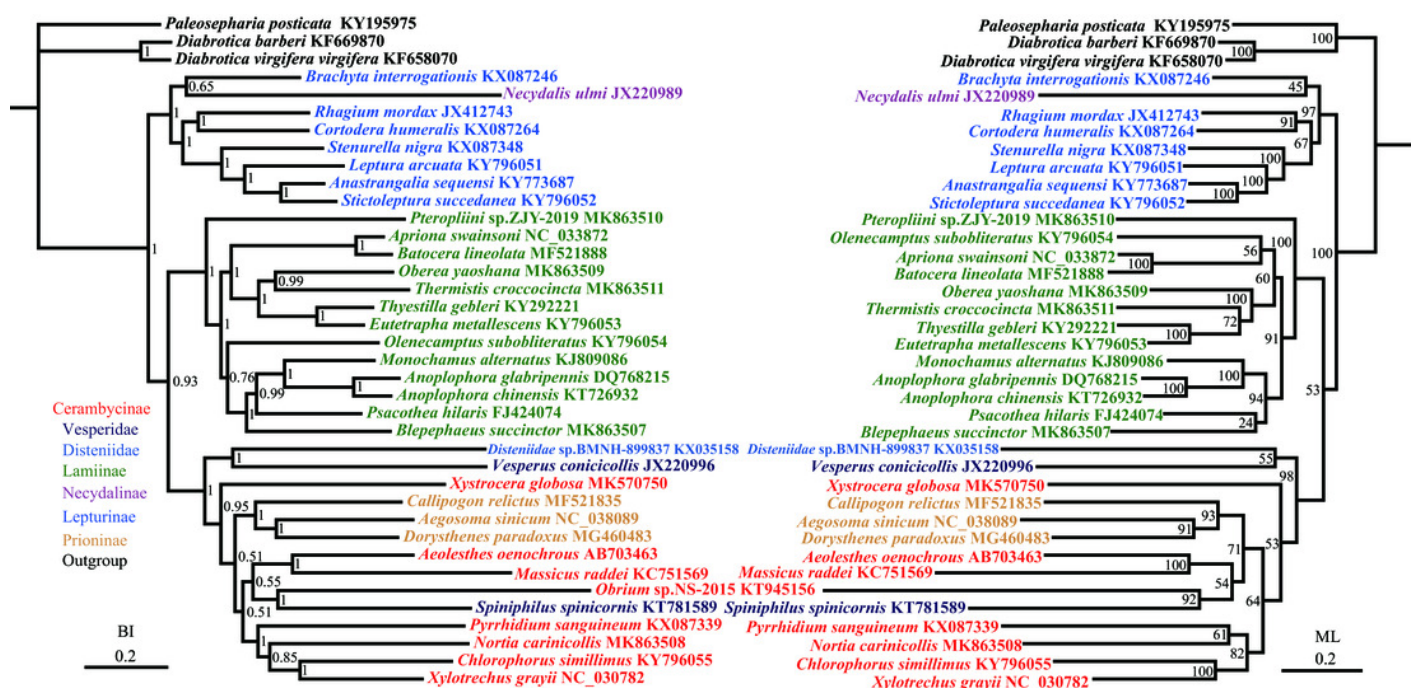
Table 1 Species used to construct the phylogenetic relationships along with GenBank accession numbers. *Partial genome.

Table 1 Species used to construct the phylogenetic relationships along with GenBank accession numbers. *Partial genome.

Order	Family	Species	GenBank No.	References
Cerambycidae	Lamiinae	*Anoplophora glabripennis*	DQ768215	Fang et al., 2016
		Psacothea hilaris	FJ424074	Kim et al., 2009
		Thyestilla gebleri	KY292221	Yang et al., 2017
		Monochamus alternatus	KJ809086	Li et al., 2016a
		Anoplophora chinensis	KT726932	Li et al., 2016b
		Apriona swainsoni	NC_033872	Que et al., 2019
		Batocera lineolata	MF521888	Liu et al., 2017
		Oberea yaoshana	MK863509	This study
		Thermistis croccocincta	MK863511	This study
		Blepephaeus succinctor	MK863507	This study
		Pterolophia sp.ZJY-2019	MK863510	This study
		Olenecamptus subobliteratus*	KY796054	Directly submitted
		Eutetrapha metallescens*	KY796053	Directly submitted
	Cerambycinae	*Xylotrechus grayii*	NC_030782	Guo et al., 2016
		Xystrocera globosa	MK570750	Wang et al., 2019
		Nortia carinicollis	MK863508	This study
		Massicus raddei	KC751569	Wang et al., 2014
		Aeolesthes oenochrous	AB703463	Chiu et al., 2016
		Obrium sp. NS-2015	KT945156	Song et al., 2017
		Pyrrhidium sanguineum*	KX087339	Directly submitted
		Chlorophorus simillimus*	KY796055	Directly submitted
	Prioninae	*Callipogon relictus*	MF521835	Lim et al., 2017
		Dorysthenes paradoxus	MG460483	Liu et al., 2018
		Aegosoma sinicum	NC_038089	Directly submitted
	Lepturinae	*Leptura arcuata**	KY796051	Directly submitted
		Stictoleptura succedanea*	KY796052	Directly submitted
		Rhagium mordax*	JX412743	Directly submitted
		Stenurella nigra*	KX087348	Directly submitted
		Cortodera humeralis	KX087264	Directly submitted
		Anastrangalia sequensi	KY773687	Directly submitted
		Brachyta interrogationis	KX087246	Directly submitted
	Necydalinae	*Necydalis ulmi**	JX220989	Directly submitted
Disteniidae	Disteniinae	*Disteniinae* sp. BMNH 899837	KX035158	Directly submitted
Vesperidae	Philinae	*Spiniphilus spinicornis*	KT781589	Nie et al., 2017
	Vesperinae	*Vesperus conicicollis**	JX220996	Directly submitted
Chrysomelidae	Galerucinae	*Paleosepharia posticata*	KY195975	Wang et al., 2017
		Diabrotica barberi	KF669870	Brad, 2014
		Diabrotica virgifera	KF658070	Brad, 2014

Table 2. The partition schemes and best-fitting models selected of 13 protein-coding genes in the 13P26 dataset.

Table 2. The partition schemes and best-fitting models selected of 13 protein-coding genes in the 13P26 dataset.

1   **Table 2.** The partition schemes and best-fitting models selected of 13 protein-coding genes in 13P26 data

Nucleotide sequence alignments		
Subset	**Subset Partitions**	**Best Model**
Partition 1	atp6_pos1, cox1 pos 1, cox2_pos1, cox3_pos1, cytb_pos1	GTR+I+G
Partition 2	atp6_pos2, cox1_pos2, cox2_pos2, cox3_pos2, cytb_pos2, nd3_pos2	TVM+I+G
Partition 3	atp8_pos1, atp8_pos2, nd2_pos2, nd3_pos3, nd6_pos2	GTR+I+G
Partition 4	nd1_pos1, nd4l_pos1, nd4_pos1, nd5 pos1	GTR+I+G
Partition 5	nd1_pos2, nd4_pos2, nd4l_pos2, nd5_pos2	GTR+I+G
Partition 6	nd2_pos2, nd3_pos2, nd6_pos2	TVM+I+G

Table 3. The partition schemes and best-fitting models selected of 12 protein-coding genes in the 12P38 dataset.

Table 3. The partition schemes and best-fitting models selected of 12 protein-coding genes in the 12P38 dataset.

1   **Table 3.** The partition schemes and best-fitting models selected of 12 protein-coding genes in 12P38 data.

Nucleotide sequence alignments		
Subset	**Subset Partitions**	**Best Model**
Partition 1	atp6_pos1, cox2_pos1, cox3_pos1, cytb_pos1	GTR+I+G
Partition 2	atp6_pos2, cox2_pos2, cox3_pos2, cytb_pos2, nd3_pos2	TVM+I+G
Partition 3	atp8_pos1, atp8_pos2, nd6_pos2	HKY+G
Partition 4	cox1 pos 1	SYM+G
Partition 5	cox1_pos2	F81+G
Partition 6	nd1_pos1, nd4l_pos1, nd4_pos1, nd5 pos1	GTR+I+G
Partition 7	nd1_pos2, nd4_pos2, nd4l_pos2, nd5_pos2,	GTR+I+G
Partition 8	nd3_pos1, nd6_pos1	GTR+I+G

Table 4 Base composition of Cerambycidae mitochondrial genomes.

Table 4 Base composition of Cerambycidae mitochondrial genomes.

Species	A+T(%)				AT-skew				GC-skew			
	Mito	PCGs	rRNAs	AT-rich region	Mito	PCGs	rRNAs	AT-rich region	Mito	PCGs	rRNAs	AT-rich region
O. yaoshana	79.1	77.8	81.1	87.1	0.03	0.14	0.04	0.04	0.20	0.01	0.38	0.24
T. croccocincta	76.4	76.4	78.6	87.4	0.15	0.15	0.04	0.04	0.13	0.01	0.49	0.45
B. succinctor	75.3	73.2	78.6	86.2	0.023	0.17	0.06	0.02	0.26	0.02	0.39	0.32
N. carinicollis	73.2	71.1	75.7	80.3	0.10	0.17	0.16	0.07	0.18	0.03	0.36	0.21
Pterolophia sp.ZJY-2019	76.7	75.1	81.7	82.8	0.02	0.18	0.02	0.04	0.22	0.04	0.36	0.18